*Larhyss Journal, ISSN 1112-3680, n°60, Dec 2024, pp. 151-169*


# MODEL SIMULATION OF DRY STORMWATER DETENTION POND WITH IPCC AR6 PROJECTED CLIMATE CHANGE SCENARIOS

***MAH D.Y.S.[1*], ALHADI H.F.[2,3], BATENI N.[4], TEO F.Y.[5]***

[1]Associate Professor, UNIMAS Water Centre, Faculty of Engineering, Universiti Malaysia Sarawak, 94300 Kota Samarahan, Sarawak, Malaysia

[2] PhD Candidate, Faculty of Engineering, Universiti Malaysia Sarawak, 94300 Kota Samarahan, Sarawak, Malaysia

[3] Director, Perunding Amal Teknik Sdn. Bhd., Kenyalang Park, 93300 Kuching, Sarawak, Malaysia

[4] Senior Lecturer, UNIMAS Water Centre, Faculty of Engineering, Universiti Malaysia Sarawak, 94300 Kota Samarahan, Sarawak, Malaysia

[5] Professor, Faculty of Science and Engineering, University of Nottingham Malaysia, 43500 Semenyih, Selangor, Malaysia

*(*) ysmah@unimas.my*

Research Article – Available at http://larhyss.net/ojs/index.php/larhyss/index
Received February 16, 2024, Received in revised form November 21, 2024, Accepted November 23, 2024

## ABSTRACT

Dry detention ponds are good practices for stormwater management that control flow discharge by temporarily storing water and gradually releasing it with no permanent water ponding. A real-life dry stormwater detention pond in Sarawak, Malaysia, was selected for this study. The pond has a dimension of 80 (length) × 10 (top width) × 1.98 (depth) $m^3$. The inlet is the end of a drain extended from a local government complex with a 27,800-$m^2$ catchment area, and the outlet is an orifice with a 0.45-m diameter. The pond is characterized by a storage volume of 1,050 $m^3$ based on a 30-min, 100-year average recurrent interval design storm. Another characteristic of the pond is the flow restriction imposed by the orifice outlet, in which water levels are always higher behind the orifice. The dry detention pond was tested against Intergovernmental Panel on Climate Change (IPCC) AR6 future scenarios by simulating catchments, adjacent drainage networks, and dry ponds with orifices using a stormwater management model. Maximum 1-day precipitation data were extracted from IPCC-WG1 Atlas according to AR6 future scenarios and periods. The data were normalized to 30-min rainfall temporal patterns. With the modelling, three hydraulic indicators were identified: water level, flow, and velocity. The high water level caused by the orifice outlet influenced the pond's water

levels. The expected rise of the pond's water levels to the extent of overflowing was ruled out. Instead, water levels were maintained below the pond-full level due to the orifice. Besides, the ponding effect during the filling of the pond's storage volume increased inflows from climate change-induced storms. The findings showed that the flow rates within the pond reduced gradually from the inlet to the outlet. Among the three indicators, only velocities along the length of the pond showed significant responses to AR6 future scenarios. The velocities increased in SSP2-4.5, SSP3-7.0, and SSP5-8.5, which calls for new solutions to the erosion of earthen pond walls.

**Keywords**: Drainage, Dry pond, MSMA, Shared Socioeconomic Pathway (SSP), Sustainable development, Storm Water Management Model (SWMM), Urban runoff.

## INTRODUCTION TO DRY STORMWATER DETENTION POND

A dry stormwater detention pond, or simply dry pond, is a large structure constructed by excavating a trench in the ground. Fig. 1 shows the selected dry pond for a case study. It is dry most of the time, except when it rains. Stormwater runoff, which is generated from rainwater falling on adjacent catchments, was directed to fill the pond and progressively released through an outlet. The dry pond should capture and temporarily store runoff (Thomsen et al., 2020; Lim et al., 2022). With the mentioned controlled releases of runoff, a stormwater management goal of reducing the peak runoff from a land development could be achieved.

Besides, the dry pond could be easily merged into urban green spaces. Malaysian town planning has designated 10% of the gross area of physical land development as reserve green spaces for recreational, sports and aesthetics purposes. In line with this development, the dry pond could be multi-functional, for example, as playground, football field, garden or others during normal weather conditions and water pond after storms. As such, the dry pond has become a popular choice of stormwater control.

In this article, we describe the case study of dry pond, in which investigative modelling was performed to illustrate the impacts of climate change on water patterns. The study site is a local government complex in Samarahan, near Kuching City, the capital of Sarawak, Malaysia. The large dry pond highlighted in Fig. 1 has dimensions of 80 (length) × 10 (top width) × 1.98 (depth) $m^3$. The pond's storage volume is 1,050 $m^3$, which caters for the runoff volume from 27,800 $m^2$ (28 hectares) of the catchment area with a time of concentration of 30 min, subjected to 96.3 mm of rainfall depth (equivalent to 100-year average recurrent interval (ARI) design storm). The pond's outlet is equipped with an orifice of 0.45 m in diameter.

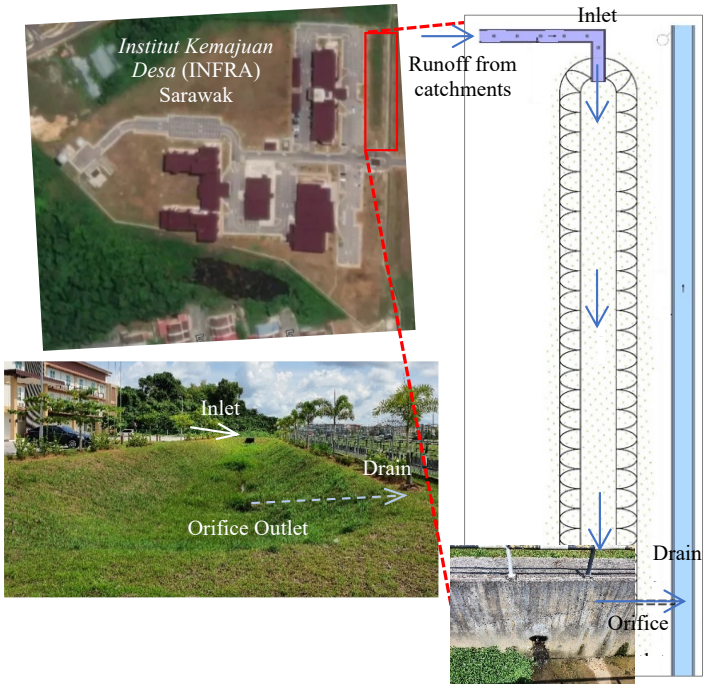


**Figure 1: Selected Dry Pond**

## CLIMATE CHANGE SCENARIOS

The Intergovernmental Panel on Climate Change (IPCC) rolled out Assessment Report 6 (AR6) in August 2021. AR6 introduces a new set of future scenarios called the Shared Socioeconomic Pathway (SSP), which is a change from the previous Assessment Report 5 (AR5) scenarios called the Representative Concentration Pathway (RCP) (Pirani et al., 2024).

The five new future scenarios for AR6 are

a) SSP1-1.9: as the most optimistic scenario, in which global $CO_2$ emissions are cut to net zero by 2050 and global warming is kept around 1.5°C above preindustrial temperatures until 2100;

b) SSP1-2.6: as the next best scenario, in which global $CO_2$ emissions are cut to net zero after 2050 and the average temperatures rise 1.8°C by 2100;

c) SSP2-4.5: as a middle-of-the-road scenario, in which global $CO_2$ emissions are cut but do not reach net zero and the average temperatures rise 2.7°C by 2100;

d) SSP3-7.0: as a dangerous scenario, in which global $CO_2$ emissions are doubled and the average temperatures rise 3.6°C by 2100;

e) SSP5-8.5: as an avoid-at-all-cost scenario, in which global $CO_2$ emissions are doubled by 2050 and the average temperatures rise 4.4°C by 2100.

After the release of AR6, the agency in charge of climate change which is the Malaysian Meteorological Department had announced the projected climatic data in different regions of Malaysia. Sarawak, in which this case study took place, was forecasted to have increases in the ground surface temperatures which are +1.35 – 1.43 °C by 2050, and +1.94 – 2.05 °C by 2100. The ranges of annual rainfall data were projected to increase which are +420 mm (12%) by 2050, and +567 mm (16%) by 2100. Other than that, the average sea level rise over the coastal of Sarawak was projected to increase as well, which is +0.72 m by 2100. However, the SSP scenario for these projections was not specified.

Sarawak, which is classified as being Tropical climate zone, is officially stated as having annual rainfall between 3,300 and 4,600 mm. The amount of rainfall is much higher than other regions of Malaysia. However, with the projected additional 12 – 16% of rainfall from AR6, it foresees an increase of flooding in the region. In fact, the detection of rainfall trends is vital (Benkhaled et al., 2008; Zeggane et al., 2021; Chadee et al., 2023). In the urban areas, stormwater drainage system is at the forefront of being tested with the higher amount of rainfall. Failing to accommodate the additional rainfall in the drainage system would cause overflowing of floodwater which subsequently inundates the land adjacent to the drain.

Dry pond is a component of the stormwater drainage system. There is a need to investigate how well the dry pond could cope with the increases of rainfall. Responses of dry pond as a receiver of rainfall due to climate-induced rainfall trends should be studied since significant changes to the amount of rainfall could trigger certain degree of impact to the pond (Koua et al., 2019; Verma et al., 2023a; 2023b). AR6 provides a means to ensure the above-mentioned study with the availability of forecasted rainfall data.

The forecasted rainfall data could be fed to a computer-aided drainage model like Storm Water Management Model (SWMM) developed by the United States Environmental Protection Agency, to simulate the dry pond for any impacts of climate change (Mah et al., 2023a; Baudhanwala et al., 2023). Weaknesses of dry pond could be identified by studying the resulted water patterns when subjected to climate change scenarios, more over with the adverse scenarios like SSP2-4.5, SSP3-7.0 and SSP5-8.5. Improvement to the dry pond design could be formulated thereafter.

With climate change in the picture, Younger et al. (2022) anticipated that the predicted rising equatorial rainfall would pose challenges to civil engineering works, including stormwater facilities. Li and Fang (2021) ran the AR5 scenarios of RCP 2.6, 4.5, and 8.5 in the Mekong Basin, Southeast Asia. The average annual precipitation is expected to increase by 8.9%, 12.8%, and 13.9% in the 2060s, and the runoff by 10.5%, 20.1%, and 23.2% during 2020–2093 under the three RCP scenarios, respectively. Yang et al. (2022) ran the same three scenarios in Chaohu City, China; as a result, the hydraulic performance of stormwater facilities declined under all scenarios, and runoff volume and peak flow

were mitigated by 45%–80% and 39%–60%, respectively. Kamagate et al. (2017) were interested in the Agnedby watershed, located southeast of Côte d'Ivoire, which has been vulnerable to climate change manifested by an increased sensitivity to extreme situations (floods and drought) since the 70s. The authors proposed modelling the flows for a water balance assessment. To achieve this, data of precipitation, evapotranspiration and runoff discharge collected over the 1984-2009 period were ejected in the GR4J model to assess its performance in runoff simulating.

However, studies based on AR6 scenarios are inadequate. Therefore, we explore the possibilities of stormwater ponds under AR6 scenarios in this study.

Examples of future climate scenarios predicted using the SWMM are essential in the study of climate change. Alamdari et al. (2020) reported the use of SWMM in which three scenarios—a historical scenario and two AR5 scenarios—were applied using RCP 4.5 and 8.5 precipitation data to project runoff and pollutant transport of total suspended solids, total nitrogen, and total phosphorous.

Wang et al. (2021) reported the use of a SWMM for a single AR5 scenario by applying RCP 8.5 climate data to project changes in the runoff volume and peak flow of bioretention systems over their life cycles. Rosenberger et al. (2021) also reported the use of a SWMM by applying RCP 8.5 climate data to project the infiltration, runoff, and storage of stormwater control structures for 2040–2069.

## MATERIAL AND METHODS

A flow chart showing the materials and methods being adopted in this study is presented Fig. 2. The centrepiece of the chart is the model building of dry pond in SWMM. To allow the setting up of the dry pond model, two main data groups were acquired. Firstly, data related to the dry pond are described the next sub-section, in which the study site provided the physical properties of the pond and since it is a real-life pond, its related technical design steps were obtained. Secondly, data related to the climate change are presented in the subsequent sub-section. At the end of this section, the modelling approach is described.

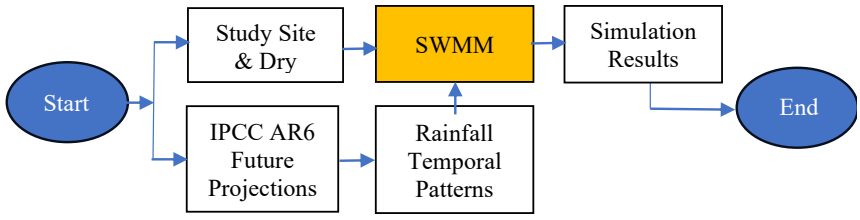


**Figure 2: Flow Chart of Methods**

**Dry pond design**

The Urban Stormwater Management Manual for Malaysia (DID, 2012) is a local manual for hydrological and hydraulic analyses involved in developing a dry pond in Malaysia. It is assumed that peak runoff occurs when all catchment parts receive rainfall and contribute to the runoff. This condition is met when the duration of the storm equals the time of concentration. In general, runoff can be estimated using a rational method:

$$Q_c = \frac{C\,.\,I\,.\,A_C}{360} \tag{1}$$

where

$Q_c$ = catchment flow ($m^3/s$),

$C$ = runoff coefficient (unitless),

$I$ = design storm (mm/hr), and

$A_C$ = catchment area (ha).

The local manual recommended a 100-year ARI design storm for a dry pond. In this case study, the catchment discharged its runoff to a drain network. The usually concrete drain design can be described by the Manning formula:

$$Q_d = \frac{1}{n}\,.\,A_d\,.\,R^{2/3}.\,{S_d}^{1/2} \tag{2}$$

where

$Q_d$ = channel flow ($m^3/s$),

$n$ = Manning's roughness coefficient based on construction material (unitless),

$A_d$ = channel flow area ($m^2$),

$R$ = hydraulic radius of channel (m), and

$S_d$ = channel slope (m/m).

With the catchment and drain parameters identified, the time of concentration can be estimated as follows:

$$t_c = t_o + t_d \tag{3}$$

where

$t_c$ = time of concentration (minute),

$t_o$ = catchment overland flow time (minute), and

$t_d$ = drain flow time from the most remote drainage inlet to the point of design (minute).

Specific to the case study, the time of concentration was estimated to be 30 min. Therefore, the storm duration was also taken as 30 min. The 30-min, 100-year ARI design storm was estimated to be 96.3 mm. The generated runoff from the design storm, after

traveling through the catchment and drain lengths, was eventually discharged into the dry pond. The water balance of the pond due to runoff flowing in and out can be estimated as follows:

$$St = \sum_i (Q_i - Q_0)\, \Delta t_s \quad (4)$$

where
$St$ = storage volume ($m^3$),
$Q_i$ = inflow ($m^3/s$),
$Q_o$ = outflow ($m^3/s$), and
$t_s$ = storm duration (s).

In this case study, inflow to the pond, $Q_i$, occurred at the endpoint of the drain network before the dry pond. The outflow, $Q_o$, that occurred due to the orifice outlet restriction can be estimated as follows:

$$Q_o = C_d \,.\, A_0 \,.\, \sqrt{2\, g\, H_o} \quad (5)$$

where

$Q_o$ = orifice flow ($m^3/s$),
$C_d$ = orifice discharge coefficient (unitless),
$A_o$ = area of orifice opening ($m^2$),
$g$ = acceleration due to gravity ($m/s^2$), and
$H_o$ = effective head on the orifice measured from the centroid of the opening (m).

**IPCC AR6 future projections**

Myhre et al. (2019) maintained that the frequency of heavy precipitation events imposed large societal effects. In urbanized catchments, this would affect the design, operation, and maintenance of urban stormwater facilities. For a small catchment (less than 80 hectares), urban stormwater facilities are usually designed to withstand precipitation events within 24 hours. Therefore, in the context of climate change, the application of a maximum 1-day precipitation is practical in urban stormwater management. Such data were provided by litterature under AR6 scenarios. The data are presented in Fig. 3, which showcases the 5$^{th}$ and 95$^{th}$ percentiles of predicted 1-day precipitation for Southeast Asia. In line with the concept of heavy precipitation, the estimated 100-year ARI design storm (96.3 mm) is superseded by the predicted 95$^{th}$ percentile data as the maximum 1-day precipitation (116–131.3 mm). Compared with the conventional 100-year ARI design storm, climate change will increase precipitation by 20%–36%.

**Rainfall temporal patterns**

Temporal patterns for design rainfall entail the most intense burst of rainfall within a storm event with respect to time and space (Houichi, 2017). These are also outlined in another local manual, Hydrological Procedure No 26 (HP26) (DID, 2018). This manual is specific to the Malaysian regions of Sabah and Sarawak, in which our study site is located.

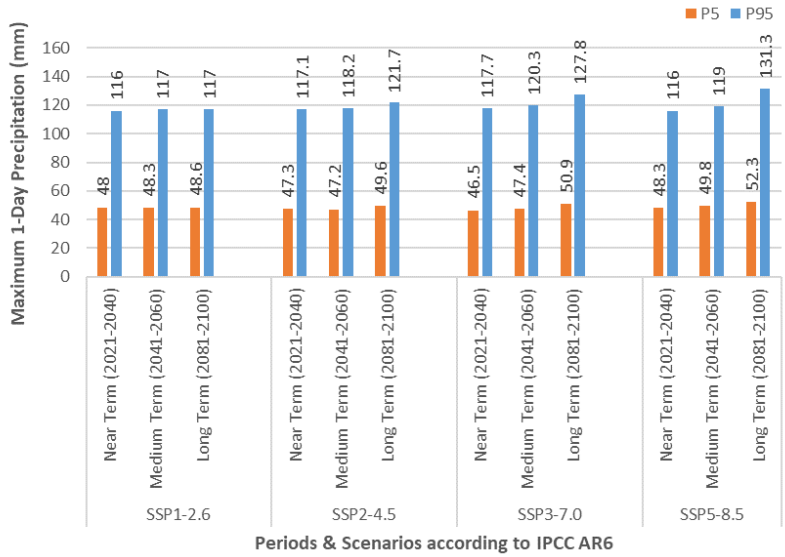


**Figure 3: Maximum 1-day precipitation according to AR6 periods and scenarios**

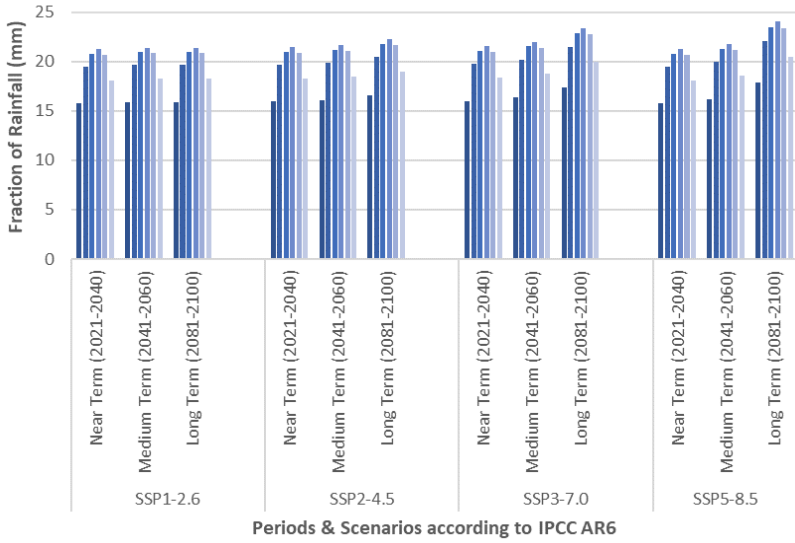


**Figure 4: Fraction of maximum 1-day precipitation according to AR6 periods and scenarios**

Recalling the assumption made in the rational method that peak flow occurs when the storm duration equals the time of concentration, the estimated 30-min time of concentration was adopted as the design storm duration. In the case study, HP26 recommended a temporal pattern of six fractions over 30 min for the estimated 100-year ARI design storm. Each fraction shared 5 min of the design storm intensity. Besides, HP26 recommended a climate change factor of 1.23. As a result, the future 100-year ARI design storm was estimated to be 118.4 mm.

The maximum 1-day precipitation data were the possible total precipitation in a day which it may happen at any time frames within the day. The assumption being made here, the potential amount of 1-day precipitation data was cramped into a very intense 30 min following the 100-year ARI design storm duration described in the previous paragraph. The resulting temporal rainfall patterns from the maximum 1-day precipitation are shown in Fig. 4. The patterns exhibit a bell-shaped distribution. The fractions of rainfall data were then input into a computer model to simulate water patterns flowing through the selected dry pond under different AR6 scenarios.

**Modelling approach**

SWMM version 5.0 (SWMM5) was employed to investigate the impacts of climate change on the selected pond subjected to IPCC AR6 projections. The heart of SWMM5 is the rainfall–runoff relationship at a site (Mah et al., 2023b). The modelling started with rainfall (Fig. 5). The rainfall temporal patterns for 100-year and future 100-year ARI design rainfalls, followed by four AR6 scenarios in near (2021–2040), medium (2041–2060), and long (2081–2100) terms, were input.

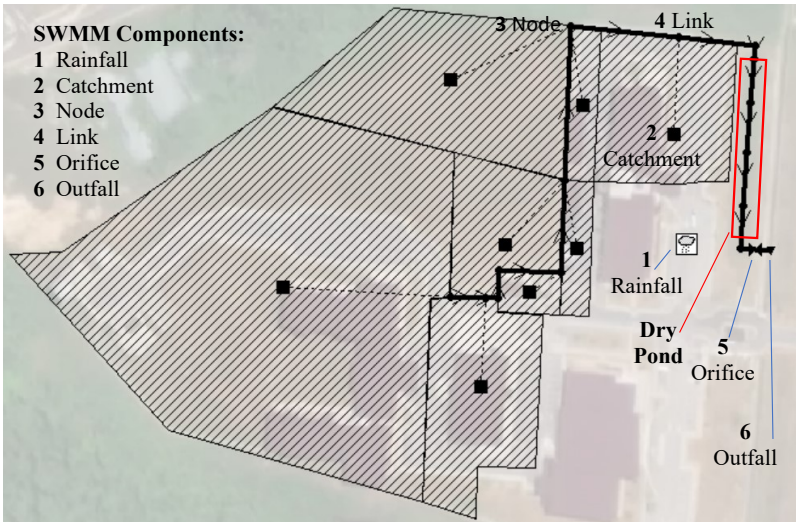


**Figure 5: Developed SWMM**

From the rainfall, SWMM5 applied a nonlinear differential equation of sheet flow to generate runoff based on the associated catchment characteristics:

$$Q_a = W\frac{1.49}{n}\left(d - d_p\right)^{5/3} S_C{}^{1/2} \quad (6)$$

where
$Q_a$ = catchment flow ($m^3/s$),
$W$ = catchment width (m),
$Sc$ = catchment slope (m),
$n$ = Manning's roughness value (unitless),
$d_p$ = maximum depression storage (m), and
$d$ = depth of water over the catchment (m).

Once the runoff flowed from the catchment to a node, SWMM5 routed the running water from node to node through a link connecting the upstream and downstream nodes until the water reached an endpoint called outfall. The dry pond can also be represented as nodes and links (Mah et al., 2020; Bentalha, 2023). The routing algorithm is given by the following kinematic wave approximation:

$$Q_b = \frac{\partial A}{\partial t} + \alpha m A^{(m-1)}\frac{\partial A}{\partial x} \quad (7)$$

where
$Q_b$ = routed drain flow ($m^3/s$),
$A$ = cross-sectional area of the drain ($m^2$),
$x$ = distance along the flow path (m),
$\delta t$ = time step (s),
$\alpha$ = flow geometry due to drain (unitless), and
$m$ = surface roughness of drain (unitless).

**Model verification**

As stated in the previous paragraph, the dry pond was represented as nodes and links, meaning it was modelled as a conduit rather than a storage unit. Therefore, the critical water flow routing through the developed dry-pond conduit was based on kinematic wave approximation method in the SWMM engine (Equation 7). On another hand, the dry pond as a conduit, it was comprised of channel compartments and orifice restrictors which their formulas are presented in Equation 2 and Equation 5, respectively. Model verifications were carried out by comparing the data from the three mentioned equations (Fig. 6).

Fig. 6a illustrates an overestimation of channel flow by the Manning equation. This was expected as the equation did not consider how the flow is affected by the orifices. The few outliers in Fig. 6a were water patterns around the orifices that produced abrupt higher flow rates than other channel stretches. On the other hand, Fig. 6b shows the model exhibits a tendency to generate higher values for orifice flow. However, the scattered plots are close to the theoretical data sets. Nevertheless, the coefficient of determination, $R^2$ values derived from both the flows through channel and orifice surpassed 0.9,

demonstrating the model's capacity to provide reasonable estimation of flows for both channel and orifice.

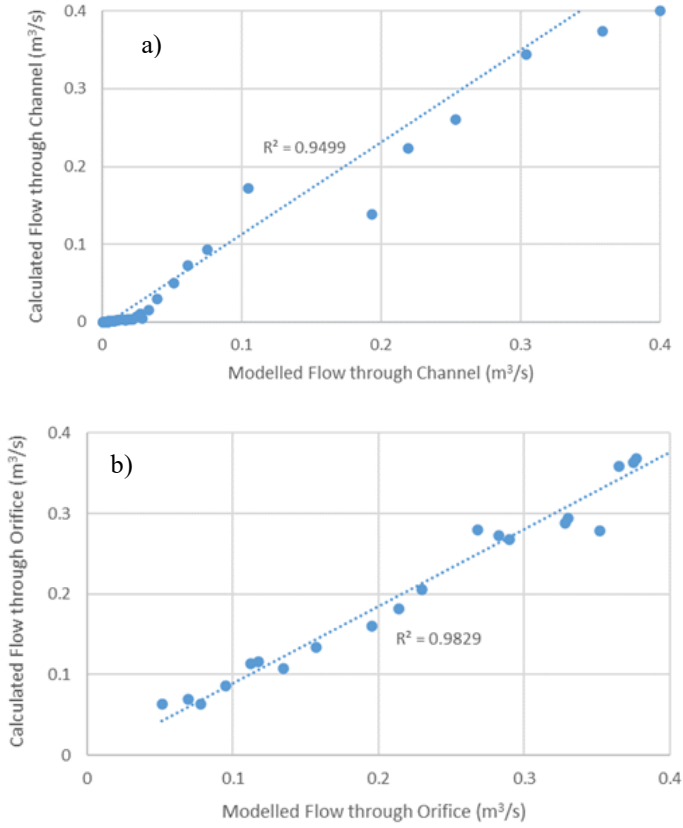


**Figure 6. Calculated vs modelled flows through, a) Channel and b) Orifice**

## RESULTS AND DISCUSSION

### Simulation of pond filling

SWMM5 could explain the dry pond's water patterns. Thus, we simulated the filling of the selected dry pond, i.e., the endpoint of the drain before the pond functions as an inlet. Runoff from the catchment was discharged to the dry pond via the inlet. From the dry pond, runoff was discharged to a major drain via an orifice outlet. The mechanism was similar to a water-draining tank receiving and discharging water synchronously.

Through 100-year ARI design storm modelling, the generated runoff reaching the pond was predicted with a peak water level of 1.35 m. Further modelling of the future 100-year ARI design storm and four AR6 future scenarios, the model predicted a range of peak water levels as 1.36–1.4 m (below the maximum depth of 1.98 m; Fig. 7). The peak water levels were found to be constant. The increments were small, only 0.7%–4% compared with the 100-year ARI design storm.

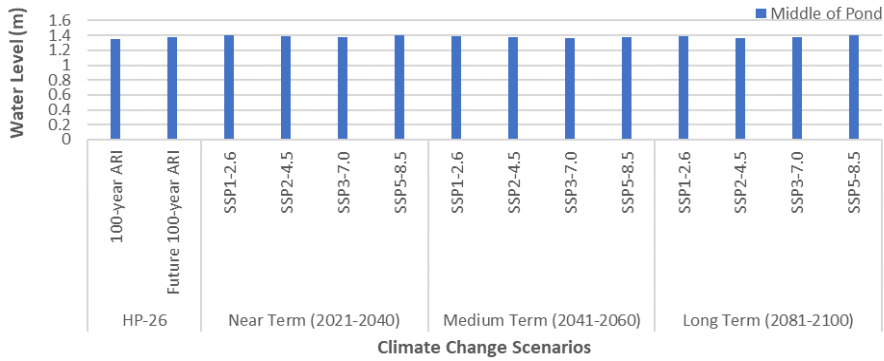


**Figure 7: Modelled peak water levels**

The dry pond could sustain floodwater in all scenarios. No overflowing was predicted; the orifice played a significant role in this phenomenon. The pond's water levels were maintained due to the orifice outlet restriction, which occurred when the outflows were maintained at approximately 0.2–0.3 $m^3/s$. This is consistent with the report of Goorden et al. (2021) that the outflow of a pond was capped at a fixed value. This occurrence could be explained as follows: while the runoff passes through an orifice from a pond, a contraction of the flow area occurs. The volume of the accelerating water is pushed back, resulting in relatively higher water levels behind the orifice.

A visualization of the pond filling is shown in Fig. 8, which illustrates the conditions in the dry pond at 10, 20, 30, and 40 min after the 100-year ARI design storm onset. The water levels were generally constant along the 80 m-length of the pond at each time frame (Fig. 8b–8d), and reached their peak at 40 min. It took 6 hours for the pond to be empty. The other scenarios exhibited similar pond filling patterns (as evident in Fig. 7); hence, we excluded them.

**Flow**

The flows varied at the pond inlet, outlet, and middle. The flow distributions are shown in Fig. 9. In general, the flow decreased when the water drained from the inlet to outlet.

**Velocity**

Peak velocities were maintained in the range of 0.40–0.45 m/s (Fig. 10). Peaks occurred near the inlet.

**Discussion**

Climate change-induced rainfall temporal patterns were reflected in the heightened inflows into the dry pond. Compared with the 100-year ARI design storm that produced an inflow of 1.52 $m^3/s$, AR6 scenarios produced inflows in the range of 1.35–1.88 $m^3/s$, which is a 24% increase. With the increased inflow, one would expect the pond to overflow. However, this was not predicted by the model. This finding refutes the contrary common belief that larger ponds are needed in addressing climate change.

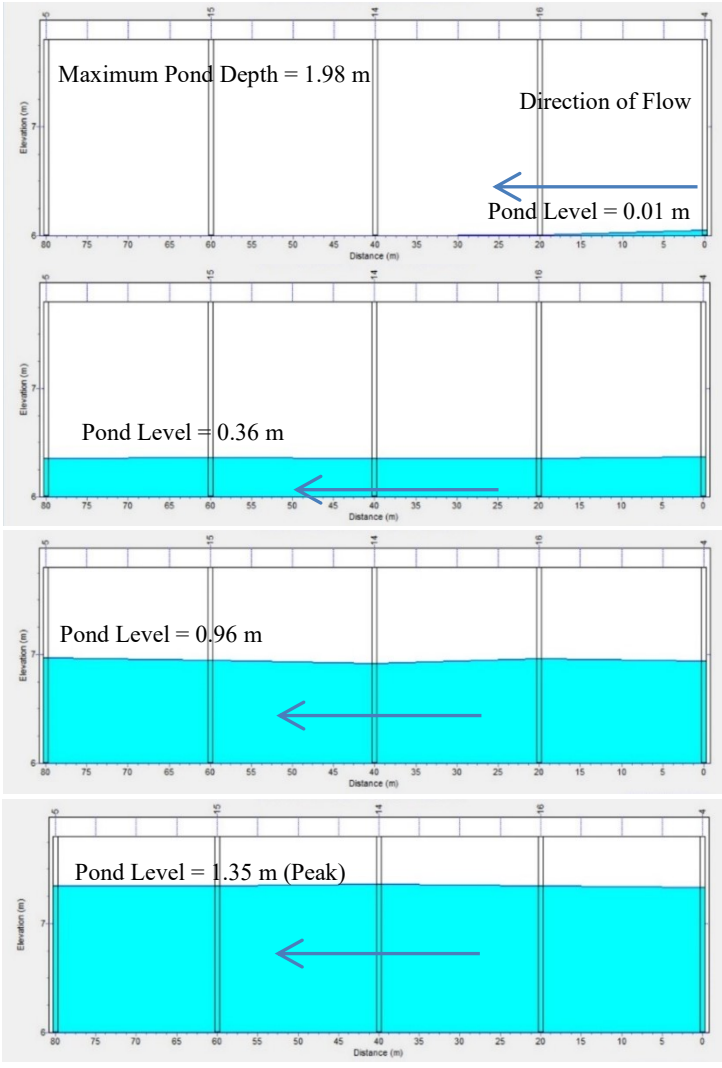


**Figure 8: Long section of pond filling at a) 10, b) 20, c) 30, and d) 40 min after the 100-year ARI design storm onset**

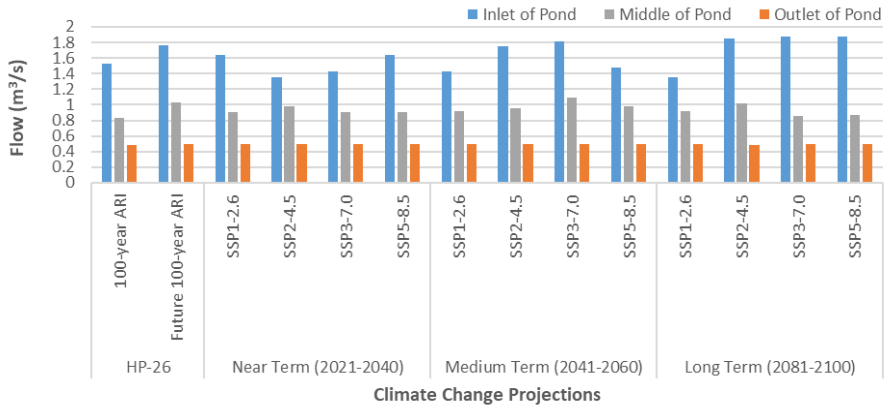


**Figure 9: Modelled flows**

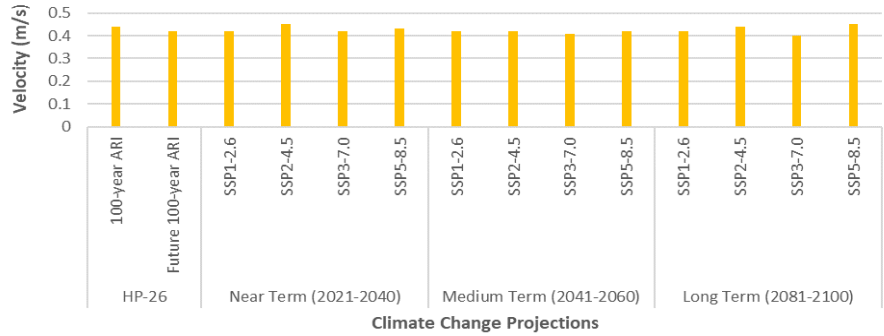


**Figure 10: Modelled peak velocities**

Runoff rates in the pond diminished from the inlet to the outlet. The outflows were much lower than the inflows. The associated velocities in the pond followed the same trend. Fig. 11 shows similar velocity patterns.

In general, the velocities demonstrated declining patterns as the running waters migrated from the inlet to the outlet. Comparisons between the AR6 scenarios indicated that the velocity patterns along the dry pond length increased for SSP2-4.5, SSP3-7.0, and SSP5-8.5 (Fig. 11b, 11c, and 11d, respectively). Using the graph line produced by the 100-year ARI design storm as the control scenario, the near and long terms' lines were above the control for higher velocities for SSP2-4.5 and SSP3-7.0. Moreover, the long term's line for SSP5-8.5 had the highest predicted velocity.

The impact of climate change was insignificant on the water levels because they were constant due to the restriction imposed by orifice, and the ponding effects due to the big storage volume of the dry pond. These findings agree with the reports of Wissler et al.

(2020). The only impact was on the heightened velocities. The increases in the pond's water velocities were alarming. The velocities may erode the earthen pond, which requires a new set of solutions.

**Limitation**

Short-duration storms (5–30 min) are meant to test the immediate response of a system in receiving a high volume of rainwater. In this case, a dry pond is safe against flooding when subjected to climate change-induced rainfall temporal patterns. This claim is only true for events with up to 30-min storm duration. A dry pond has not been tested with long-duration storms. The endurance of dry ponds against climate change should be further investigated with events of 24-, 48- and 72-hour storm durations.

a)

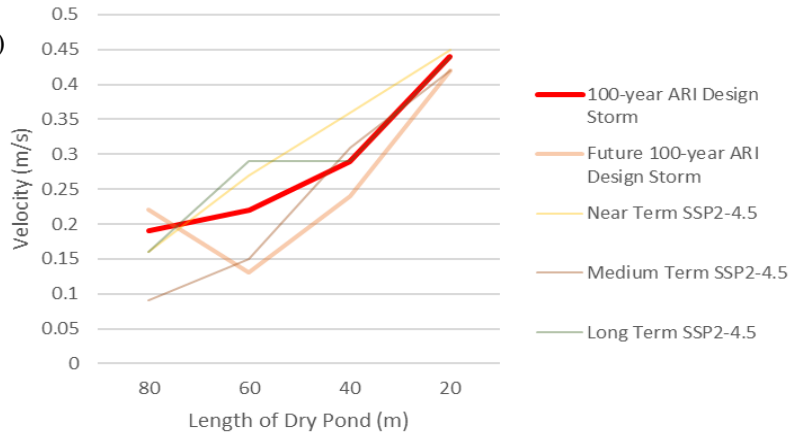


b)

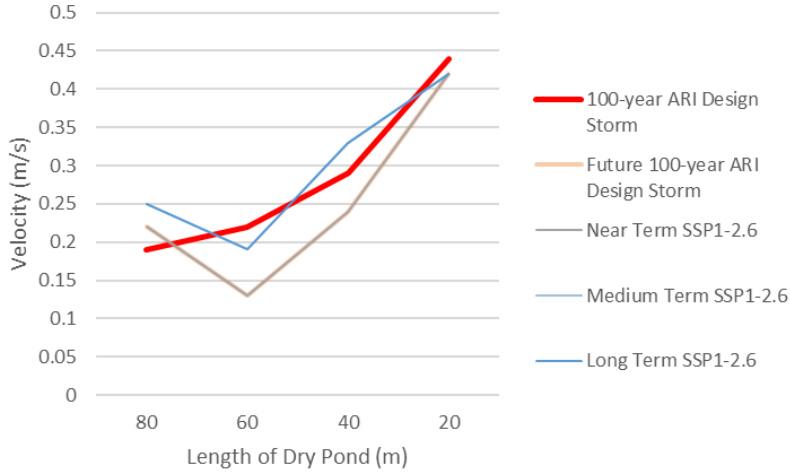

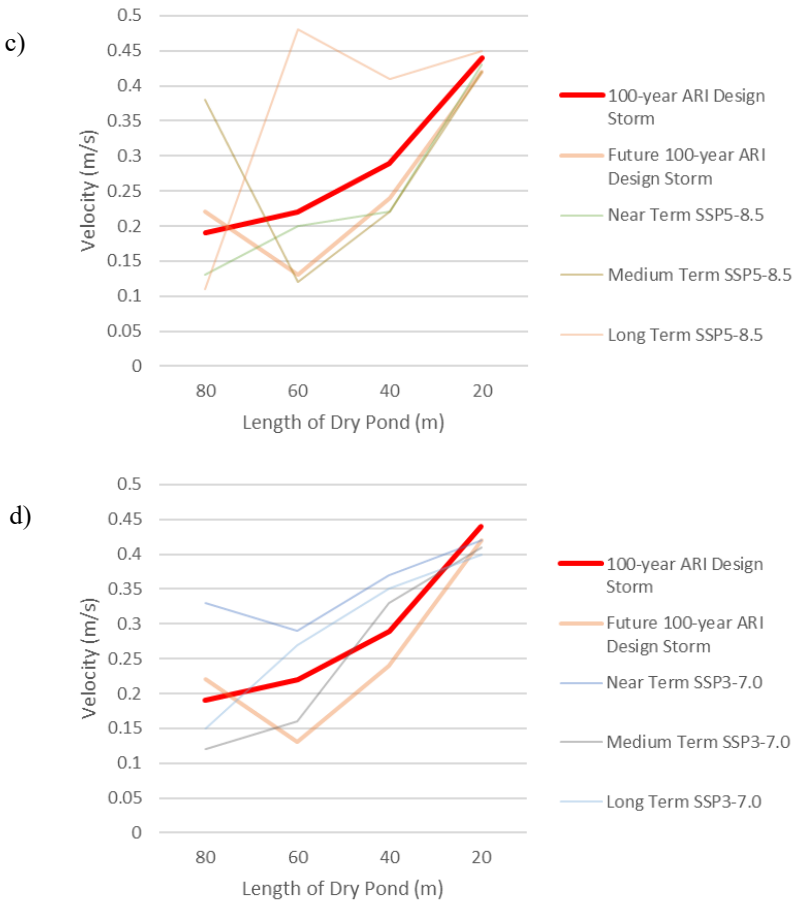


**Figure 11: Velocities along the length of dry pond according to AR6 scenarios, a) SSP1-2.6, b) SSP2-4.5, c) SSP3-7.0, and d) SSP5-8.5**

## CONCLUSION

The presented modelling efforts were made to provide insights into the water patterns of a single dry pond. Three hydraulic indicators were highlighted: the pond's water level, the associated flow being discharged into the pond, and the resulting velocities along the 80-m-long pond.

First, we found that the water outflow restriction due to the orifice was prominent. Owing to a single orifice, the running waters were pushed back, resulting in constant water levels behind the orifice. The impact of climate change on the pond's water levels was insignificant.

Second, while the running waters were in motion, flow data at the pond inlet, middle, and outlet were collected. We found that the flows were high in the inlet vicinity. The flows then slowed down as they continued to the middle and outlet. The volume of water entering the pond experienced a ponding effect that explained the diminished flow rates. Thus, the impact of climate change on the pond's flow was also insignificant.

Third, the impact of climate change was found to prevail in the pond's velocities. Separating the velocities along the pond according to SSP1-2.6, SSP2-4.5, SSP3-7.0, and SSP5-8.5, the velocities were predicted to increase with the severity of the AR6 future scenarios.

**Declaration of competing interest**

The authors declare that they have no known competing financial interests or personal relationships that could have appeared to influence the work reported in this paper.

**Acknowledgment**

The authors would like to thank Universiti Malaysia Sarawak for providing the financial support via the GRADUATES grant (Project ID: UNI/F02/GRADUATES/85186/2022).

## REFERENCES

ALAMDARI N., SAMPLE D.J., ROSS A.C., EASTON Z.M. (2020). Evaluating the impact of climate change on water quality and quantity in an urban watershed using an ensemble approach, Estuaries and Coasts, Vol. 43, No 1, pp. 56-72. https://doi.org/10.1007/s12237-019-00649-4.

BAUDHANWALA D., KANTHARIA V., PATEL D., MEHTA D., WAIKHOM, S. (2023). Applicability of SWMM for urban flood forecasting a case study of the western zone of Surat City, Larhyss Journal, No 54, pp. 71-83.

BENKHALED A., BOUZIANE M.T, ACHOUR B. (2008). Detecting trends in annual discharge and precipitation in the Chott Melghir basin in southeastern Algeria, Larhyss Journal, No 7, pp. 103-119.

BENTALHA C. (2023). Evaluation of the hydraulic and hydrology performance of the green roof by using SWMM, Larhyss Journal, No 53, pp. 61-72.

CHADEE A., NARRA M., MEHTA D., ANDREW J., AZAMATHULLA H.M. (2023). Impact of climate change on water resource engineering in Trinidad and Tobago, Larhyss Journal, No 55, pp. 215-229.

DEPARTMENT OF IRRIGATION AND DRAINAGE MALAYSIA (DID) (2012). Urban Stormwater Management Manual for Malaysia, 2nd Edition, ISBN 978-983-9304-24-4.

DEPARTMENT OF IRRIGATION AND DRAINAGE MALAYSIA (DID) (2018). Hydrological Procedure No 26 (HP26): Estimation of Design Rainstorm in Sabah and Sarawak (Revised and Updated 2018), ISBN 978-983-9304-49-7.

GOORDEN M.A., LARSEN K.G., NIELSEN J.E., NIELSEN T.D., RASMUSSEN M.R., SRBA J. (2021). Learning safe and optimal control strategies for storm water detention ponds, IFAC-Papers online, Vol. 54, No. 5, pp. 13-18. https://doi.org/10.1016/j.ifacol.2021.08.467.

HOUICHI L. (2017). Appropriate formula for estimating rainfall intensity of selected duration and frequency: a case study, Larhyss Journal, No 30, pp. 67-87. (In French)

KAMAGATE B., DAO A., NOUFE D., YAO K.L., FADIKA V., GONE D.L., SAVANE I. (2017). Contribution of GR4J model for modeling Agne by watershed runoff in southeast of Côte d'Ivoire, Larhyss Journal, No 29, pp. 187-208.

KOUA T., ANOH K., EBLIN S., KOUASSI K., KOUAME K., JOURDA J. (2019). Rainfall and runoff study in climate change context in the Buyo lake watershed (southwest Côte d'Ivoire), Larhyss Journal, No 39, pp. 229-258. (In French)

LI C., FANG H. (2021). Assessment of climate change impacts on the streamflow for the Mun River in the Mekong Basin, Southeast Asia: using SWAT model, CATENA, Vol. 201, Paper ID 105199. https://doi.org/10.1016/j.catena.2021.105199.

LIM J.S., TAN C.Y., MAH Y.S., LEE M.L., TEO F.Y. (2022). Numerical modelling of urban stormwater management with grassed road divider as bioretention system, 2nd International Conference on Civil and Environmental Engineering, E3S Web of Conferences., Vol. 347, Paper ID 04007. https://doi.org/10.1051/e3sconf/202234704007. https://doi.org/10.184000/tjce.1310648.

MAH D.Y.S., DAYANG NUR HUWAIDA A.S., TEO F.Y. (2023a). Investigation of historical extreme rainfall on permeable road in a commercial centre, Larhyss Journal, No 53, pp. 165-182.

MAH D.Y.S., BATENI N., PUTUHENA F.J. (2023b). Case study of stormwater control by permeable road in commercial centre under equatorial climate, Turkish Journal of Civil Engineering, Vol. 34, No. 4, pp. 133-142.

MAH D.Y.S., NGU J.O.K., TAIB S.N.L., MANNAN M.A. (2020). Modelling of compartmentalized household storm water detention system using SWMM5, International Journal of Emerging Trends in Engineering Research, Vol. 8, No 2, pp. 344-349. https://doi.org/10.30534/ijeter/2020/17822020.

MYHRE G., ALTERSKJÆR K., STJERN C.W., HODNEBROG Ø., MARELLE L., SAMSET B.H., SILLMANN J., SCHALLER N., FISCHER E., SCHULZ M., STOHL A. (2019). Frequency of extreme precipitation increases extensively with event rareness under global warming, Scientific Reports, Vol. 9, No 1, Paper ID 16063. https://doi.org/10.1038/s41598-019-52277-4.

PIRANI A., FUGLESTVEDT J.S., BYERS E., O'NEILL B., RIAHI K., LEE J.Y., MAROTZKE J., ROSE S.K., SCHAEFFER R., TEBALDI C. (2024). Scenarios in IPCC assessments: lessons from AR6 and opportunities for AR7, npj Climate Action, Vol. 3, No 1, pp. 1-7. https://doi.org/10.1038/s44168-023-00082-1.

ROSENBERGER L., LEANDRO J., PAULEIT S., ERLWEIN S. (2021). Sustainable stormwater management under the impact of climate change and urban densification, Journal of Hydrology, Vol. 596, Paper ID 126137. https://doi.org/10.1016/j.jhydrol.2021.126137.

THOMSEN A.T.H., NIELSEN J.E., RIIS T., RASMUSSEN M.R. (2020). Hydraulic effects of stormwater discharge into a small stream, Journal of Environmental Management, Vol. 270, Paper ID 110793. https://doi.org/10.1016/j.jenvman.2020.110793.

VERMA S., KUMAR K., VERMA M.K., PRASAD A.D., MEHTA D., RATHNAYAKE U. (2023a). Comparative analysis of CMIP5 and CMIP6 in conjunction with the hydrological processes of reservoir catchment, Chhattisgarh, India, Journal of Hydrology: Regional Studies, Vol. 50, Paper ID 101533. https://doi.org/10.1016/j.ejrh.2023.101533.

VERMA S., VERMA M.K., PRASAD A.D., MEHTA D., AZAMATHULLA H.M., MUTTIL N., RATHNAYAKE U. (2023b). Simulating the hydrological processes under multiple land use/land cover and climate change scenarios in the Mahanadi reservoir complex, Chhattisgarh, India, Water, Vol. 15, Issue 17, Paper ID 3068. https://doi.org/10.3390/w15173068.

WANG M., ZHANG D., WANG Z., ZHOU S., TAN S.K. (2021). Long-term performance of bioretention systems in storm runoff management under climate change and life-cycle condition, Sustainable Cities and Society, Vol. 65, Paper ID 102598, https://doi.org/10.1016/j.scs.2020.102598.

WISSLER A.D., HUNT W.F., MCLAUGHLIN R.A. (2020). Hydrologic and water quality performance of two aging and unmaintained dry detention basins receiving highway stormwater runoff, Journal of Environmental Management, Vol. 255, Paper ID 109853, https://doi.org/10.1016/j.jenvman.2020.109853.

YANG W., ZHANG J., KREBS P. (2022). Low impact development practices mitigate urban flooding and non-point pollution under climate change, Journal of Cleaner Production, Vol. 347, Paper ID 131320. https://doi.org/10.1016/j.jclepro.2022.131320.

YOUNGER S., PARRY D., MEIGH D. (2022). Preparing for the future: the impact of climate change on the civil engineering profession, Proceedings of the Institution of Civil Engineers: Civil Engineering, Vol. 175, No. 2, pp. 87-93. https://doi.org/10.1680/jcien.21.00174.

ZEGGANE H., GHERNAOUT R., BOUTOUTAOU D., ABDULLAH S.S., REMINI B., KISI O. (2021). Multidimensional analysis of precipitation in central-northern region of Algeria, Larhyss Journal, No 47, pp. 209-231.